Eur. Phys. J. A **29**, 151–159 (2006)
DOI 10.1140/epja/i2006-10084-x

THE EUROPEAN PHYSICAL JOURNAL A

Spin-parity measurements in the neutron-rich N $\sim$ 20 ^{34}P and ^{36}S nuclei

Krishichayan[1], A. Chakraborty[1,a], S. Mukhopadhyay[1], S. Ray[1], N.S. Pattabiraman[1,b], S.S. Ghugre[1,c], R. Goswami[1], A.K. Sinha[1], S. Sarkar[2], U. Garg[3], P.V. Madhusudhana Rao[3], S.K. Basu[4], B.K. Yogi[5], L. Chaturvedi[6], A. Dhal[6], R.K. Sinha[6], M. Saha Sarkar[7], S. Saha[7], R. Singh[8], R.K. Bhowmik[9], A. Jhingan[9], N. Madhavan[9], S. Muralithar[9], S. Nath[9], R.P. Singh[9], and P. Sugathan[9]

[1] UGC-DAE Consortium for Scientific Research, Kolkata Centre, Sector III/LB-8, Bidhan Nagar, Kolkata 700 098, India
[2] Department of Physics, The University of Burdwan, Burdwan 713 104, India
[3] Department of Physics, University of Notre Dame, Notre Dame, IN 46556, USA
[4] Variable Energy Cyclotron Centre, Sector-I/AF, Bidhan Nagar, Kolkata 700 064, India
[5] Department of Physics, Govt. College, Kota 324 009, India
[6] Department of Physics, Banaras Hindu University, Varanasi 221 005, India
[7] Saha Institute of Nuclear Physics, Sector-I/AF, Bidhan Nagar, Kolkata 700 064, India
[8] Department of Physics and Astrophysics, University of Delhi, New Delhi 110 007, India
[9] Nuclear Science Centre, Aruna Asaf Ali Marg, New Delhi 110 067, India

Received: 5 January 2006 / Revised: 5 July 2006 /
Published online: 6 September 2006 –
Communicated by J. Äystö

Abstract. Yrast and near-yrast energy levels in the neutron-rich $N \sim 20$ nuclei ^{34}P, ^{36}S were populated using transfer/deep-inelastic processes following the ^{34}S + ^{115}In reaction at an incident energy of 140 MeV. The use of a multi-clover array has facilitated polarization measurements of the observed γ-rays and necessitated some changes in the previously known level scheme. The observation of the negative-parity levels in these nuclei on the periphery of the "island of inversion" is indicative of the influence of the intruder orbitals on the level structure at low spins. Shell-model calculations indicate that the inclusion of the orbitals from the upper pf shell is important even for the low-lying positive-parity states.

PACS. 23.20.Lv Gamma transitions and level energies – 23.20.En Angular distribution and correlation measurements – 21.60.Cs Shell model – 27.30.+t $20 \leq A \leq 38$

1 Introduction

The exploration of the nuclear structure of neutron-rich nuclei in the difficult to access $A \sim 30$–40 mass region has revealed several intriguing aspects even at low spins *viz*, deformation, shape coexistence etc. [1,2]. There are theoretical predictions for variation in the spin-orbit strength as a function of the neutron number for these neutron-rich nuclei. Relativistic mean-filed calculations by G.A. Lalazissis *et al.* [3] have indicated a considerable reduction in the magnitude of the spin-orbit interaction potential for the light drip-line nuclei. With the increase of neutron number, the effective one-body spin-orbit interaction becomes weaker, resulting in a smaller energy splitting between the spin-orbit partners. Further, it has been observed, for example, that the neutron-rich $N = 20$ Na and Mg isotones exhibit anomalous behavior in their binding energies [1,4]. The results indicate that these nuclei are more bound than the predictions of the shell-model calculations within the *sd* major shell. These $N = 20$–22 Ne, Na and Mg isotopes, form the so-called "island of inversion": a small region of the nuclear landscape [5] where the ground state consists of intruder configurations $\nu(sd)^{N-2}\nu(pf)^2$. The normal states, which do not involve such excitations, usually occur at much higher excitation energies. An interesting observation is the occurrence of the first-excited 2^+ state in ^{32}Mg at a remarkably low excitation-energy of 885 keV [2], unexpected for this $N = 20$ closed-shell nucleus. This is clearly indicative of the onset of deformation and $B(E2, 0^+ \rightarrow 2_1^+)$ measurements [6] confirm the occurrence of a considerable deformation in this nucleus. These observations provide tantalizing hints for the disappearance of the $N = 20$ magic structure for the $Z \leq 12$ nuclei.

[a] *Present address:* Department of Physics, Krishnath College, Berhampore 742 101, India.
[b] *Present address:* Department of Physics, University of York, York YO10 5DD, UK.
[c] e-mail: ssg@alpha.iuc.res.in

Here, the *sd* and *pf* shells come closer, making them softer towards dynamical deformation, leading to the aforementioned anomalous properties. The occurrence of low-lying intruder states has been attributed to the residual inter- and intra-shell strong interactions [5,7]. These many-body correlations tend to reduce the shell gaps, thus stabilizing the deformed intruder configurations at a much lower excitation energy.

Since these nuclei are not easily accessible using the conventional fusion-evaporation reactions, the available information on the level structure is limited. The heavy-ion multi-nucleon transfer process provides an alternative method to populate these neutron-rich nuclei. In fact, several authors [8] have demonstrated the power of heavy-ion induced transfer reactions for selective population of near-yrast high-spin states. This feature has also made it possible to undertake a detailed investigation of the subsequent decay properties of these states. Thick-target measurements [9–12] have successfully established the level structure of ^{34}P and ^{36}S up to $E_x \sim 5$ MeV. In the present study, these nuclei have been populated by heavy-ion transfer reactions. In order to establish the spins and parities of the observed levels, we have employed an array of Compton-suppressed Clover detectors. These detectors provide a unique opportunity to undertake linear polarization measurements to establish the parity of the observed levels. We present here our experimental results which confirm the spin and parity assignments of the observed levels in ^{36}S and suggest a change in the parity of the level at 2305 keV in ^{34}P. These results are compared with the predictions of large-basis shell-model calculations. The influence of the intruder orbitals on the structure of the levels in these nuclei is discussed.

2 Experimental methods and results

The $^{34}\mathrm{S} + ^{115}\mathrm{In}$ reaction at an incident beam energy of 140 MeV was carried out using the 15 UD Pelletron facility at the Nuclear Science Centre, New Delhi. The experiment was optimized to investigate high-spin states in $N \sim 82$ nuclei, *e.g.*, ^{146}Tb [13] via fusion-evaporation reactions. However, it was expected that the same reaction would also populate projectile-like neutron-rich nuclei following the transfer of a few nucleons. The isotopically enriched ^{115}In target of $\sim 1.29\,\mathrm{mg/cm^2}$ thickness with a $\sim 7.14\,\mathrm{mg/cm^2}$ Au backing was used. The de-exciting γ-rays were detected using INGA (Indian National Gamma Array), comprising of 8 Compton-suppressed Clover detectors. The detectors were placed at 80° and 140° with respect to the beam direction. A total of about 220 million two- or higher-fold γ-γ coincidence events were recorded. The data were pre-sorted to correct for any on-line drifts [14], precisely gain-matched [15], and were sorted into symmetric and angle-dependent matrices for detailed off-line analysis. The data were analyzed using IUCSORT [16,17] and RADWARE [18] analysis packages.

The results include the observation of γ-ray cascades up to the highest-known yrast states in ^{34}P and ^{36}S. The angle-dependent matrices were successfully used to obtain

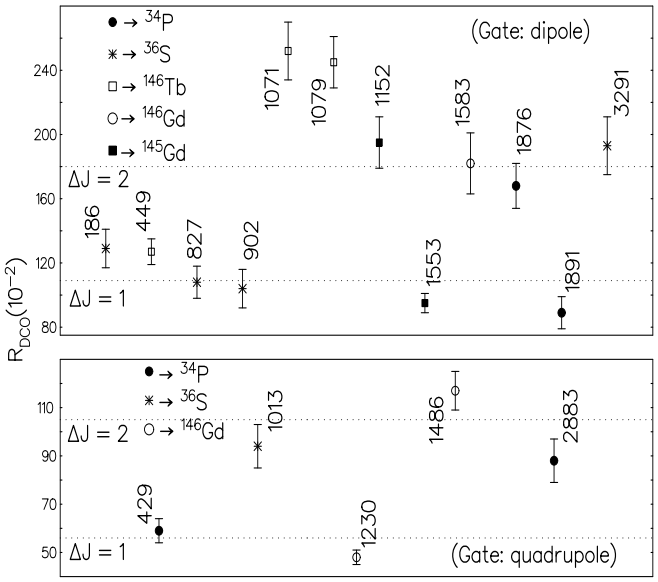

Fig. 1. γ-ray anisotropy ratio R_{DCO}, for the transitions belonging to ^{34}P and ^{36}S. For comparison, the corresponding values of a few known transitions belonging to ^{146}Tb, ^{145,146}Gd populated via the fusion channel, are also shown. The dotted lines correspond to the average values obtained for the known dipole ($\Delta J = 1$) and quadrupole ($\Delta J = 2$) transitions while gated by dipole (top panel) and quadrupole (bottom panel) transitions. These lines have been drawn to guide the eye. The quoted error includes error due to background subtraction, peak fitting, and efficiency correction.

information on the multipolarities of the known transitions for the nuclei populated via the fusion-evaporation channel, *viz* ^{145,146}Tb using the procedures described in refs. [13,19,20]. The observed values of R_{DCO} (gated on known dipole as well as quadrupole transitions) are illustrated in fig. 1.

Several authors (see, for example, ref. [21]) have demonstrated the feasibility of extending this procedure to nuclei populated following transfer and multi-fragmentation process (non-equilibrated reactions). The γ-ray anisotropy ratio for transitions belonging to these neutron-rich projectile-like nuclei such as ^{36}S, ^{34}P are depicted in fig. 1. As seen from the figure, the results are very similar to those obtained for nuclei populated following the conventional fusion-evaporation reactions. The details of these measurements are provided in table 1.

The use of Clover detectors facilitated polarization measurements [22–24]. In a Clover detector, each of the individual crystals is considered as a scatterer, while the two adjacent crystals as the observers. The anisotropy between the number of Compton scattered γ-rays in the reaction plane $N_{\parallel}$, and perpendicular to it, $N_{\perp}$, is indicative of the electromagnetic nature of the transition. Even though the statistics in the present data permitted only qualitative polarization estimates, these in conjunction with the coincidence angular correlation measurements were crucial

Table 1. Gamma transition energy (E_γ) in keV, excitation energy (E_x) in keV, initial and final spins for the transitions, relative intensity (I_γ), DCO and IPDCO ratio for the γ-ray transitions and assigned multipolarity in ^{36}S and ^{34}P.

E_γ	E_x	$J_i^\pi \rightarrow J_f^\pi$	I_γ	R_{DCO}		Δ_{IPDCO}	Multipolarity
(keV)	(keV)			Gate: dipole	Gate: quadrupole		
^{36}S							
185.5	5206.0	$5^- \rightarrow 4^-$	53.9(5.7)	1.29(0.12)			$M1$
760.4	5780.9		14.0(2.5)	dipole			dipole
827.3	5020.5	$4^- \rightarrow 3^-$	61.4(6.0)	1.08(0.10)		−0.16(0.17)	$M1$
902.4	4193.2	$3^- \rightarrow 2^+$	100	1.04(0.12)		0.06(0.08)	$E1$
1012.8	5206.0	$5^- \rightarrow 3^-$	14.4(2.7)		0.94(0.09)	electric	$E2$
3290.8	3290.8	$2^+ \rightarrow 0^+$	> 100	1.93(0.18)		0.11(0.13)	$E2$
^{34}P							
429.3	429.3	$2^+ \rightarrow 1^+$	> 155		0.59(0.05)	−0.16(0.13)	$M1$
1179.1	1608.4	$(1^+) \rightarrow 2^+$	17.1(1.1)	dipole			($M1$)
1875.9	2305.2	$4^+ \rightarrow 2^+$	100	1.68(0.14)		0.15(0.17)	$E2$
1891.2	2320.5	$3^- \rightarrow 2^+$	38.5(1.8)	0.89(0.10)		0.16(0.17)	$E1$
2883.0	5188.2	$6^- \rightarrow 4^+$	16.1(1.1)		0.88(0.09)	−0.22(0.11)	$M2$

for the assignment of the spins and parities of the observed levels.

A polarization matrix was constructed from the data where the energy recorded in any detector was placed on one axis, while the other axis corresponded to the energy scattered in a perpendicular or parallel segment of the Clover with respect to the beam axis. From the projected spectra, the number of perpendicular ($N_\perp$) and parallel ($N_\parallel$) scatters for a given γ-ray could then be obtained. The asymmetry parameter Δ_{IPDCO} is defined as

$$\Delta_{IPDCO} = \frac{(a(E_\gamma)N_\perp) - N_\parallel}{(a(E_\gamma)N_\perp) + N_\parallel}.$$

The correction parameter, $a(E_\gamma)$, due to the asymmetry of the detector configuration has been deduced using radioactive sources, and is expressed as a function of the γ-ray energy using the relation:

$$a(E_\gamma) = a_0 + a_1 E_\gamma,$$

where, $a_0 = 1.016(6)$ and $a_1 = -1.32(53) \times 10^{-5}\,(\text{keV})^{-1}$. P. Datta *et al.* [25] have demonstrated that the dominant correction factor, a_0, is nearly constant up to ~ 2.7 MeV.

A pure electric transition due to its preferential scattering in the perpendicular direction with respect to the beam axis results in a positive value for Δ_{IPDCO}. Similarly, a pure magnetic transition results in a negative value for Δ_{IPDCO} due to its preferential scattering along the parallel direction and a near-zero value for Δ_{IPDCO} is indicative of an admixture.

For example, the 3291 keV ($\Delta J = 2$) transition, in ^{36}S, has a preferential scattering in the perpendicular direction with respect to the beam axis, a characteristic for an electric transition. A similar pattern was observed for the 902 keV ($\Delta J = 1$) transition in the same nucleus. However, the 827 keV transition in ^{36}S, has a preferential scattering along the parallel direction with respect to the beam axis, which is indicative of a magnetic transition. These assignments are in agreement with the earlier reported values, which were based only on an angular distribution analysis. Figure 2 illustrates the asymmetry values of the observed transitions obtained from the polarization measurements. These results are also summarized in table 1. As seen from the figure, the results are identical for the nuclei populated following fusion-evaporation and those populated following few-nucleon transfer reactions. Thus, the present method, even though qualitative, demonstrates the feasibility to undertake polarization measurements for these high-energy transitions where the polarization sensitivity is low.

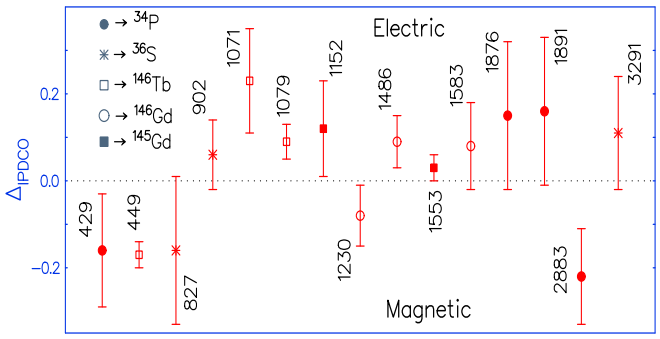

Fig. 2. Representative experimental γ-ray asymmetry parameter, from polarization measurements plotted for γ-ray transitions of ^{34}P, ^{36}S. For comparison, the corresponding values of a few known transitions belonging to ^{146}Tb, ^{145,146}Gd populated via the fusion channel are also shown. A positive value corresponds to an electric transition, while a magnetic transition results in a negative value. The quoted error encompasses errors due to background subtraction and fitting. The dotted line indicates the zero value of Δ_{IPDCO} and has been drawn to guide the eye.

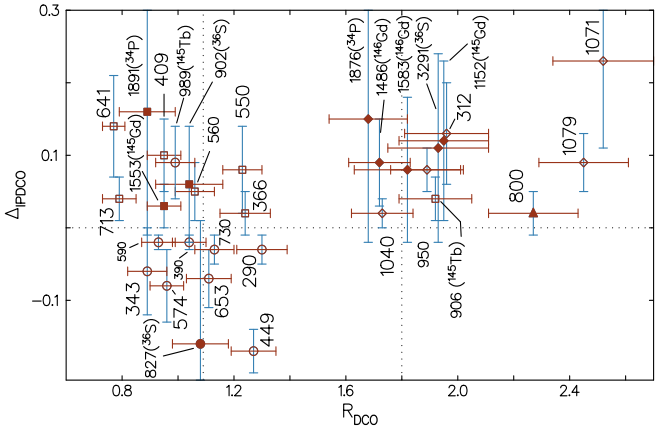

Fig. 3. Two-dimensional plot of the asymmetry parameter Δ_{IPDCO} *vs.* the angular correlation ratio R_{DCO} for nuclei populated following the $^{34}S + ^{115}In$ reaction at an incident beam energy of 140 MeV. The unmarked transitions belong to ^{146}Tb. The dotted lines parallel to the y-axis correspond to the value obtained for known dipole and quadrupole transitions, respectively. The dotted line parallel to the x-axis indicates the zero value of Δ_{IPDCO}. These lines have been drawn to guide the eye.

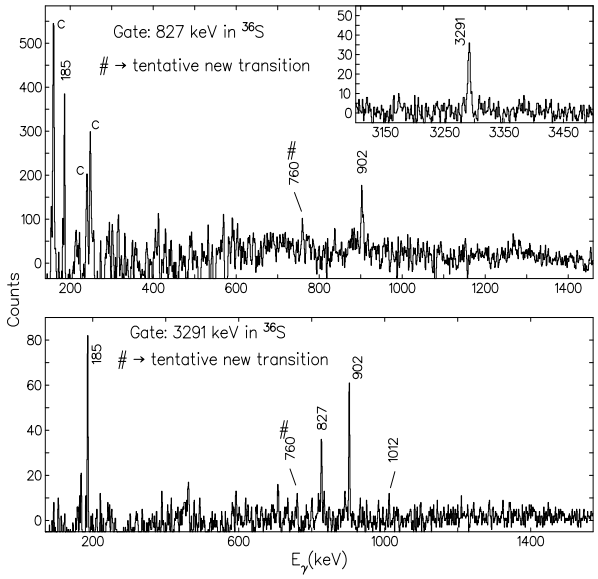

Fig. 4. Representative γ-γ coincidence spectrum with gate on the 827 and 3291 keV transitions in ^{36}S. The peaks labeled c are contaminants, either from fusion channel or from unknown origin.

The results of the coincidence angular correlation and polarization measurements are summarized in a two-dimensional plot illustrated in fig. 3. As seen from the figure, these results are qualitatively independent of the reaction mechanism and, hence, could be used to undertake the multipolarity assignments for the projectile-like neutron-rich nuclei.

2.1 ^{36}S

The level structure of $^{36}_{16}S_{20}$ has been studied by several groups in the past [9,10,26–31]. Excited states with $J^\pi = 2^+$, 3^-, 4^-, 5^-, (6^+) have been observed. The spins and parities of the observed levels have been assigned from the angular distribution analysis for the excited levels populated mainly with *deuteron*- and *triton*-induced reactions [26–30]. The ground state and the first-excited state are assigned to the $\pi(s_{1/2})^2$ and the $\pi[(d_{3/2})^1(s_{1/2})^1]$ configuration, respectively [26,28]. The negative-parity states obviously involve nucleon excitations to the next major shell (pf) across the $N = 20$ magic shell closure.

In the present experiment, ^{36}S was populated via the two-neutron pickup process. All the previously reported transitions [10] (except the 1485 keV $(6^+) \rightarrow 5^+$ transition) have been observed. Figure 4 shows two representative γ-ray coincidence spectra with gates on the 3291 $(2^+ \rightarrow 0^+)$ and the 827 $(4^- \rightarrow 3^-)$ keV transitions belonging to ^{36}S. As mentioned earlier, polarization measurements were possible for most of the observed transitions in ^{36}S. The present statistics did not permit us to undertake a polarization measurement for the 1012 keV transition.

Spin-parity assignments for the low-lying negative-parity levels are crucial. They reveal the influence of the intruder orbitals belonging to the pf shell on the structure of these apparently *sd* shell nuclei, lying close to the "island of inversion". The present polarization and angular correlation measurements confirm the J^π assignments for the 3^-, 4^- and 5^- levels.

A 760 keV γ-ray transition belonging to ^{36}S has also been observed in the present study. However, the present statistics did not permit us to undertake the angular correlation and the polarization measurements for this weak transition. Hence, the transition is tentatively placed in the level scheme (fig. 5).

To interpret the observed level structure of ^{36}S, detailed shell-model calculations have been performed using the cross-shell *sdpfmw* Hamiltonian with ^{16}O core, available with the code OXBASH [32].

Calculations were first performed within the full *sd* major shell. The ground state was found to be overbound by about 900 keV, when compared with the experimental value [5]. The predicted excitation energy of the 2^+ level is in excellent agrement with the observed value. These calculations predict that the 2^+ level is dominated by the $(1d_{5/2})^{12}$ $(1d_{3/2})^5$ $(1s_{1/2})^3$ configuration. The other positive-parity states [31] are predicted at much higher excitation energies. This indicates that even at these spins the *sd* shell-model space is inadequate to describe these states. Further, the negative-parity states cannot be generated within the *sd* shell, and excitations to the intruder pf shell have to be considered.

Hence, the model space needs to be expanded to include orbitals from the pf major shell. The valence space in this case would encompass the $1d_{5/2}$, $1d_{3/2}$, $2s_{1/2}$ and $1f_{7/2}$, $2p_{3/2}$, $2p_{1/2}$ orbitals. The interaction consisted of three parts *viz* the *sd* and pf shell interactions and the

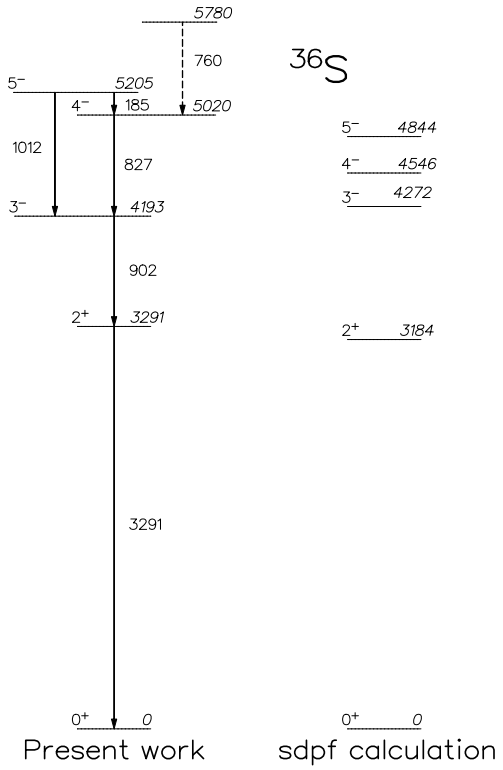

Fig. 5. The level scheme of ^{36}S for the levels populated in the ^{34}S + ^{115}In reaction. The experimental excitation energies are compared with the shell-model calculation.

cross-shell interactions. The cross-shell interaction has to effectively take into consideration the $\Delta l = 3$ component, due to the interaction between the f and s orbitals. Usually, the single-particle energies (SPEs) used in these calculations are devoid of the influence of the cross-shell interactions and have to be re-adjusted to reproduce the observed energy level spectra [31]. Unrestricted shell-model calculations are not computationally feasible with the full *sdpf* shell. Hence, the model space needs to be truncated. The truncation of the model space leads to the ground state being less bound. This also requires the adjustment of the single-particle energies.

The shell-model calculations were carried out using the $[(1d_{5/2})^{12}\ (1d_{3/2})^{0-8}\ (2s_{1/2})^{0-4}\ (1f_{7/2})^{0-2}\ (2p_{3/2})^{0-2}\ (2p_{1/2})^{0-2}]$ partitions. These partitions allow the promotion of a pair of nucleons to the $1f_{7/2}$, $2p_{3/2}$ and $2p_{1/2}$ orbitals. It was observed that lowering of the SPEs for the pf shell by about 4.5 MeV resulted in a reasonable agreement between the predicted and the observed excitation energies. The results are depicted in fig. 5 and the details are provided in table 2. The comparison is restricted only to the levels experimentally observed in the present study.

The calculations revealed that, as mentioned earlier, the ground state is indeed dominated by the configurations arising due to the excitations of nucleons within the *sd* major shell. However, configurations involving nucleons in the $1f_{7/2}$, $2p_{3/2}$, $2p_{1/2}$ orbitals also contribute to the wave function. A similar observation also holds good for the 2^+ level. Naturally, the $J^\pi = 3^-, 4^-, 5^-$ levels involve excitation of nucleons into the pf shell (see table 2).

2.2 ^{34}P

The level structure of ^{34}P, has been the focus of several investigations [9,33–37]. β-decay studies [33] identified its ground state as $J^\pi = 1^+$. The ground state and the first-excited state ($J^\pi = 2^+$ at 429 keV) in ^{34}P were suggested to be the members of a pure $(\pi s_{1/2}, \nu d_{3/2})$-multiplet. Using the ^{34}S (t, ^{3}He) ^{34}P reaction, Ajzenberg-Selove *et al.* [34] had identified states at $E_x = 2225$ and 2309 keV. Such a large energy gap is characteristic of the excitation of nucleons across a shell closure. Based on the comparison with the ^{64}Zn(t, ^{3}He)^{64}Cu reaction, where states originating from the occupation of the $1g_{9/2}$ intruder orbital were observed, they have tentatively assigned these levels as $J^\pi = 3^-$ and 4^-, respectively. These states would then correspond to the $(\pi s_{1/2} \times \nu f_{7/2})_{3^-,4^-}$-multiplet.

The observation of the level at 2305 keV was further confirmed by Fornal *et al.* [9]. They had assigned it a spin and parity of $J^\pi = 3^-$ or 4^- (see fig. 5 of [12]). They did not observe the previously reported level at 2225 keV. In a subsequent Coulomb excitation measurement, Prity-chenko *et al.* [37] have identified a level at $E_x = 2225$ keV and assigned it a spin and parity of $J^\pi = 2^+$.

Asai *et al.* [11] have reported lifetime measurements for nano-second isomers in the neutron-rich $N \sim 19$ nuclei produced by heavy-ion deep-inelastic collisions. They had assigned a limit of $0.3 \leq t_{1/2} \leq 2.5$ ns for the isomeric level at $E_x = 2305$ keV in ^{34}P. The γ-ray anisotropy analysis revealed that the 1876 keV transition which de-populated this level was a stretched quadrupole. Hence, the 1876 keV transition was assigned an $M2$ multipolarity, leading to $J^\pi = 4^-$ for the level at $E_x = 2305$ keV.

Recent measurement by Ollier *et al.* [12] have established the yrast and near-yrast excited levels of ^{34}P using the ^{36}S + ^{176}Yb reaction at an incident beam energy of 230 MeV. They have established the level scheme up to an excitation energy of $\sim$ 6.2 MeV. They have not observed the 2225 keV level reported in the Coulomb excitation measurements [37]. However, they have observed two close-lying levels at 2305 and 2320 keV. The spin-parity assignments of these levels (4^- and 3^-, respectively) are based on the energy level systematics in the neighboring nuclei. Ollier *et al.* [12] have suggested that the states above an excitation energy of 2305 keV involve intruder configurations from the pf orbitals.

All the γ-rays reported by Ollier *et al.* [12], except the 1046 keV transition, have been observed in the present study (fig. 6). It is intriguing that the 1046 keV transition, which was reported to be about 3 times more intense than the 2883 keV transition [12], could not be observed in the present investigation. A weak 1179 keV γ-ray has been observed by us which decays from a level at $E_x = 1608$ keV. This transition has also been reported in refs. [35,37].

A representative coincidence γ-ray spectrum gated on the 429 keV transition in ^{34}P is illustrated in fig. 6. Transitions (though weak) belonging to the target-like nuclei,

Table 2. Wave function compositions for the levels observed in ^{36}S and ^{34}P. In the Table, the Hamiltonian single particle states are in the following order: $1d_{5/2}$ $1d_{3/2}$ $2s_{1/2}$ $1f_{7/2}$ $1f_{5/2}$ $2p_{3/2}$ $2p_{1/2}$. Partitions used for shell-model calculation: $(1d_{5/2})^{12}(1d_{3/2})^{0-8}(2s_{1/2})^{0-4}(1f_{7/2})^{0-2}(2p_{3/2})^{0-2}(2p_{1/2})^{0-2}$.

^{36}S			^{34}P		
J^π	Wave function	Partitions (%)	J^π	Wave function	Partitions (%)
0^+	12 4 4 0 0 0 0	(70.27)	1^+	12 3 3 0 0 0 0	(76.52)
	12 2 4 2 0 0 0	(9.50)		12 1 3 2 0 0 0	(9.25)
	12 6 2 0 0 0 0	(5.93)		12 4 2 0 0 0 0	(3.77)
	12 4 2 2 0 0 0	(4.74)		12 2 2 2 0 0 0	(2.92)
	12 3 3 1 0 1 0	(3.68)		12 3 1 2 0 0 0	(2.52)
	12 2 4 0 0 2 0	(2.06)		12 2 2 1 0 1 0	(2.32)
2^+	12 5 3 0 0 0 0	(61.47)	(1_2^+)	12 4 2 0 0 0 0	(67.55)
	12 3 3 2 0 0 0	(18.20)		12 2 2 2 0 0 0	(15.69)
	12 4 2 2 0 0 0	(4.45)		12 5 1 0 0 0 0	(7.90)
	12 6 2 0 0 0 0	(3.30)		12 3 1 2 0 0 0	(5.07)
	12 4 2 1 0 1 0	(2.61)			
	12 2 4 2 0 0 0	(2.16)	2^+	12 3 3 0 0 0 0	(78.73)
				12 1 3 2 0 0 0	(9.89)
3^-	12 3 4 0 0 1 0	(68.22)		12 2 2 1 0 1 0	(3.10)
	12 4 3 1 0 0 0	(12.26)		12 3 1 2 0 0 0	(2.63)
	12 5 2 0 0 1 0	(5.06)		12 2 2 2 0 0 0	(2.48)
	12 1 4 2 0 1 0	(4.15)			
	12 3 2 2 0 1 0	(2.86)	3^-	12 2 3 1 0 0 0	(72.00)
				12 3 2 1 0 0 0	(13.47)
4^-	12 3 4 1 0 0 0	(75.06)		12 3 2 0 0 1 0	(5.31)
	12 5 2 1 0 0 0	(8.56)		12 4 1 1 0 0 0	(4.71)
	12 4 3 1 0 0 0	(6.55)			
	12 4 3 0 0 1 0	(4.04)	4^+	12 2 2 2 0 0 0	(42.61)
	12 2 3 2 0 1 0	(3.24)		12 1 3 2 0 0 0	(27.33)
				12 1 3 1 0 1 0	(11.72)
5^-	12 3 4 1 0 0 0	(76.47)		12 2 2 1 0 1 0	(9.00)
	12 5 2 1 0 0 0	(9.21)		12 1 3 0 0 2 0	(3.43)
	12 4 3 0 0 1 0	(4.44)			
	12 4 3 1 0 0 0	(4.13)	6^-	12 2 3 1 0 0 0	(88.90)
	12 2 3 2 0 1 0	(3.31)		12 3 2 1 0 0 0	(5.89)
				12 1 2 2 0 1 0	(3.20)

were also identified in coincidence. As seen from the figure, the present data is similar to the data reported in ref. [12].

The polarization measurements for the levels in ^{34}P confirmed the "electric" nature for the 1891 keV transition. The angular correlation measurements indicated that this transition involves $\Delta J = 1$ (fig. 1 and table 1). Hence, the level at $E_x = 2320$ keV is assigned as $J^\pi = 3^-$. This is in agreement with the tentative assignment of Ollier *et al.* [12]. However, for the 1876 keV ($\Delta J = 2$) transition, the polarization measurement indicated an electric nature (fig. 2). Hence, the level de-populated by this transition at $E_x = 2305$ keV is assigned as $J^\pi = 4^+$, which is in contradiction to the earlier $J^\pi = 4^-$ assignments [11,12]. Further, the measurements confirmed the magnetic nature for the 2883 keV transition. The previously reported [12] multipolarity assignment of this transition was based on the energy level systematics. The level at $E_x = 5188$ keV is now assigned as $J^\pi = 6^-$. Thus, the polarization measurements have necessitated a few changes in the previously reported level structure of ^{34}P. The level scheme obtained in this work is shown in fig. 7. The tentative multipolarity assignment for the 1179 keV transition is guided by the predictions of the shell-model calculations and corroborates the assignment as discussed in refs. [35,37].

To corroborate the linear polarization measurements, energy level systematics in this region are very crucial. These are illustrated in fig. 8. As seen from the figure, the lowest negative-parity level in ^{36}S ($J^\pi = 3^-$) occurs at $E_x = 4193$ keV [10], however, in ^{35}S, the lowest negative-parity level ($J^\pi = 7/2^-$) is observed at $E_x = 1991$ keV [9]. A similar feature is also seen in ^{37}Cl [9] and ^{36}Cl [38], and in ^{34}Si [9] and ^{33}Si [9]. The systematic observations reveal that the negative-parity sequences commence at a spin difference of about $\mid 0.5\hbar \mid$ between the $N = 20$ and 19 isotopes.

The systematics indicate that the negative-parity sequence in ^{34}P occurs at a lower excitation energy in comparison to ^{35}P ($N = 20$) and the energy difference is around 2 MeV. The negative-parity sequence in ^{35}P com-

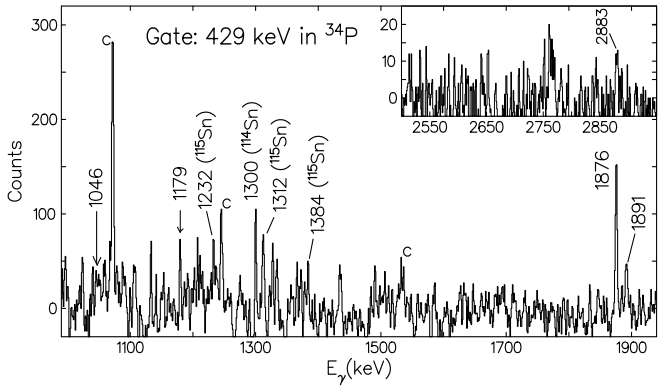

Fig. 6. Part of the γ spectrum obtained from the gate on the 429 keV transition in ^{34}P. As seen from the figure, the 1046 keV transition reported earlier has not been observed.

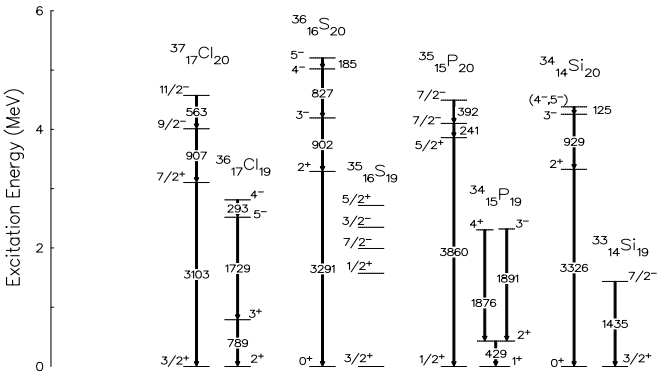

Fig. 8. Energy level systematics for $N = 20$ and 19 isotones for Cl, S, P and Si [9,10,38,39], together with the level scheme of ^{34}P from the present work.

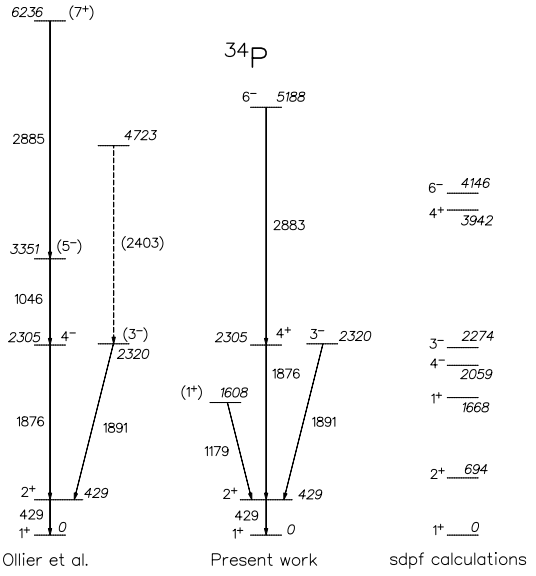

Fig. 7. A comparison of the levels in ^{34}P observed in the present work and that of Ollier *et al.* with the results of shell-model calculation. See the text for other shell-model calculations.

mences at $E_x = 4101$ keV and a spin of $J = 7/2$ [9,39]. In ^{34}P ($N = 19$), the negative-parity sequence would, then, be expected to commence around $E_x \sim 2$ MeV, and a spin of $J = 3^-$ when compared with the corresponding level in ^{35}P and supports the present $J^\pi = 3^-$ assignment for the level at $E_x = 2320$ keV. It is observed that the 4^- level in the neighboring ^{34}Si [9], ^{36}S [10] nuclei, de-excites via an $M1$ transition to the 3^- level below it. However, in ^{34}P, the level at 2305 keV is lower in excitation energy than the 3^- level, and de-excites to the 2^+ level by an $M2$ transition, if it is assigned as 4^- [11,12]. Thus, the level energy systematics do not favour the 4^- assignment for the level at 2305 keV.

Further, in ^{32}P [39], the observed 4^+ level is lower in energy compared to the 3^- level. The energy difference is around 170 keV. As seen from the present level scheme for ^{34}P, the assigned 4^+ level is indeed lower in excitation energy than the 3^- level. The marginal energy difference of about 15 keV could be attributed to the increase in the neutron number from ^{32}P to ^{34}P. Thus, this energy systematics would also favour the present 4^+ assignment.

Shell-model calculations for ^{34}P were performed within the *sd* shell using the *sdpfmw* Hamiltonian. It was observed that the ground state was over-bound by about 600 keV [5], a feature that was observed in ^{36}S as well. The 2^+ state is predicted at $E_x = 363$ keV, in reasonable agreement with the experimental value. The calculations predict an excited 1^+ level around 1408 keV.

The $(d_{5/2})^{12}$ $(s_{1/2}d_{3/2})^6$ configurations cannot generate a 4^+ state. For a completely filled $d_{5/2}$ orbital, the 4^+ could only be obtained if pf orbitals are included in the valence space. As mentioned earlier, these calculations are computationally prohibitive and hence, the model space was truncated, using the $[(1d_{5/2})^{12}$ $(1d_{3/2})^{0-8}$ $(2s_{1/2})^{0-4}$ $(1f_{7/2})^{0-2}$ $(2p_{3/2})^{0-2}$ $(2p_{1/2})^{0-2}]$ partitions. The SPEs for the pf orbitals had to be lowered by about 5.0 MeV to obtain a reasonable agreement with the observed level energies. These calculations reproduced the binding energy within 500 keV. It is worth mentioning that the lowering of the SPEs did not affect the predicted excitation energy for the 2^+ and 1_2^+ levels. The predicted 1_2^+ level occurs at 1688 keV which is very close to the experimentally observed level at 1608 keV. Therefore, the level at 1608 keV has been tentatively assigned as $J^\pi = 1^+$. The calculated energy levels are compared with the experimental levels in fig. 7 and the detailed nucleon configurations are listed in table 2. The predicted excitation energy for the 4^+ level is higher than the experimental value by about 1.5 MeV. This might be due to the truncation of the model space.

An interesting observation is that a $(\pi s_{1/2} \times \nu f_{7/2})_{3^-,4^-}$-multiplet occurs at excitation energy around 2 MeV, similar to ref. [40]. The calculations predict a 4^- level at an excitation energy of around 2 MeV. It may be tempting to assign the level at 2305 keV as a 4^- based on these calculations. However, as mentioned previously, the

polarization results are clearly indicative of a 4^+ assignment.

A sensitive test for the obtained wave functions is provided by the comparison between the predicted and the observed experimental transition probabilities. The calculated $B(E2)$'s are sensitive to the nucleon effective charges used. These calculations were performed using the effective electric charges reported by Utsuno *et al.* [7] *viz* ($e_p = 1.3e, e_n = 0.5e$). Pritychenko *et al.* have reported their calculations for $B(E2; 1^+ \rightarrow 2_1^+)$ and $B(E2; 1^+ \rightarrow 2_2^+)$ in ^{34}P [37]. Hence, the calculations were at first performed for these states. The predicted $B(E2; 1^+ \rightarrow 2_1^+)$ and $B(E2; 1^+ \rightarrow 2_2^+)$ values are 0.385 and 9.76 e^2fm^4, respectively. These are in close agreement with the values of 0.3 and 9.6 e^2fm^4 as obtained by Pritychenko *et al.* [37].

Similar calculations have also been carried out for $B(E2; 2^+ \rightarrow 0^+)$ in ^{36}S. The calculated value of 23.20 e^2fm^4 is in good agreement with the corresponding experimental result (20.8(5.6) e^2fm^4) [39]. It was observed that the set of $e_p = 1.3e$ and $e_n = 0.3e$ also reproduced well the aforementioned experimental transitional probability (within the error limit) for ^{36}S and the prediction of Pritychenko *et al.* for ^{34}P [37]. This corroborates the validity of the obtained wave functions and the choice of the effective charges.

As mentioned earlier, Asai *et al.* [11] have provided a limit ($0.3\,\text{ns} < t_{1/2} < 2.5\,\text{ns}$) for the half-life of the level at 2305 keV in ^{34}P. Based on these measurements they have assigned $J^\pi = 4^-$ to the 2305 keV level. The limits on the lifetime measurements provide a value of $0.873 \leq B(M2; 4^- \rightarrow 2^+) \leq 7.274\ \mu_N^2\text{fm}^2$. Using the present wave functions and the conventional values for the g-factors, the calculated $B(M2)$ is 8.538 μ_N^2fm^2. This is comparable to the upper limit of the corresponding experimental value. On the other hand, for a 4^+ assignment to the 2305 keV level, the experimental transition probability would be $0.01 \leq B(E2; 4^+ \rightarrow 2^+) \leq 0.117\ e^2\text{fm}^4$. The predicted transition probabilities are: $B(E2; 4^+ \rightarrow 2^+) = 0.247\ e^2\text{fm}^4$ (with $e_p = 1.30e, e_n = 0.5e$) and $B(E2; 4^+ \rightarrow 2^+) = 0.110\ e^2\text{fm}^4$ (with $e_p = 1.30e, e_n = 0.3e$). Thus, the reported experimental lifetime limit [11] cannot be used to unambiguously assign the spin and parity to the 2305 keV level in ^{34}P.

3 Conclusion

Few-nucleon transfer following the $^{34}\text{S} + ^{115}\text{In}$ reaction at an incident beam energy of 140 MeV has allowed the population of the neutron-rich $N \sim 20$ ^{36}S and ^{34}P nuclei. The spin-parity determination was made possible due to the use of an array of Clover detectors. These measurements have provided additional information on the previously established level structures of these nuclei.

The spin-parity assignments highlight the role of intruder orbitals in the structure of the observed levels. The dominant configurations of the observed levels, obtained from the shell-model calculations, demonstrate explicitly the probable importance of the intruder orbitals, even for generating the low-lying positive-parity levels.

The authors would like to thank all the participants in the joint National effort to set up the Clover array (INGA) at the Nuclear Science Centre (NSC), New Delhi. The help received from the accelerator staff at NSC is gratefully acknowledged. The help and co-operation received from our colleagues at UGC-DAE-CSR and NSC is appreciated. The authors are grateful to Professor B.A. Brown for numerous discussions. We are grateful to the Centre for Mobile Computing and Communication, Jadavpur University under the UGC Scheme "Universities with Potential for Excellence" for providing us the p-650 server computing facility. This work has been supported partially by the INDO-US, DST-NSF grant (DST-NSF/RPO-017/98) and by the U.S. National Science Foundation (grant no. INT-01115336).

References

1. C. Thibault, R. Klapisch, C. Rigaud, A.M. Poskanzer, R. Prieels, L. Lessard, W. Reisdorf, Phys. Rev. C **12**, 644 (1975).
2. C. Détraz, D. Guillemaud, G. Huber, R. Klapisch, M. Langevin, F. Naulin, C. Thibault, L.C. Carraz, F. Touchard, Phys. Rev. C **19**, 164 (1979).
3. G.A. Lalazissis, D. Vretenar, W. Pöschl, P. Ring, Phys. Lett. B **418**, 7 (1998).
4. B.H. Wildenthal, W. Chung, Phys. Rev. C **22**, 2260 (1980).
5. E.K. Warburton, J.A. Becker, B.A. Brown, Phys. Rev. C **41**, 1147 (1990).
6. T. Motobayashi *et al.*, Phys. Lett. B **346**, 9 (1995).
7. Yutaka Utsuno, Takaharu Otsuka, Takahiro Mizusaki, Michio Honma, Phys. Rev. C **64**, 011301(R).
8. P.D. Bond, J. Barrette, C. Baktash, C.E. Thorn, A.J. Kreiner, Phys. Rev. Lett. **46**, 1565 (1981); M.W. Guidry *et al.*, Phys. Lett. B **163**, 79 (1985).
9. B. Fornal *et al.*, Phys. Rev. C **49**, 2413 (1994).
10. X. Liang *et al.*, Phys. Rev. C **66**, 014302 (2002).
11. M. Asai, T, Ishii, A. Makishima, M. Ogawa, M. Matsuda, in *Proceedings of the Third International Conference on Fission and Properties of Neutron-Rich Nuclei*, edited by J.H. Hamilton, A.V. Ramayya, H.K. Carter (World Scientific, Singapore, 2002) pp. 259-265.
12. J. Ollier *et al.*, Phys. Rev. C **71**, 034316 (2005).
13. Krishichayan *et al.*, Phys. Rev. C **70**, 044315 (2004).
14. N.S. Pattabiraman, S.N. Chintalapudi, S.S. Ghugre, Nucl. Instrum. Methods Phys. Res. A **526**, 439 (2004).
15. N.S. Pattabiraman, S.N. Chintalapudi, S.S. Ghugre, Nucl. Instrum. Methods Phys. Res. A **526**, 432 (2004).
16. N.S. Pattabiraman, S.S. Ghugre, S.K. Basu, U. Garg, S. Ray, A.K. Sinha, S. Zhu, Nucl. Instrum. Methods Phys. Res. A **562**, 222 (2006).
17. N.S. Pattabiraman, S.K. Basu, S.N. Chintalapudi, U. Garg, S.S. Ghugre, S. Ray, A.K. Sinha, S. Zhu, *Abstract of the Conference on Frontiers of Nuclear Structure, Berkeley, 2002*, LBNL-50598, Abs. p. 124.
18. D.C. Radford, Nucl. Instrum. Methods Phys. Res. A **361**, 297 (1995).
19. F.S. Stephens, M.A. Delenplanque, R.M. Diamond, A.O. Macchiavelli, J.E. Draper, Phys. Rev. Lett. **54**, 2584 (1985).

20. C.W. Beausang, D. Prévost, M.H. Bergström, G. de France, B. Haas, J.C. Lisle, Ch. Theisen, J. Timár, P.J. Twin, J.N. Wilson, Nucl. Instrum. Methods Phys. Res. A **364**, 560 (1995).
21. F. Azaiez, Nucl. Phys. A **704**, 37c (2002); F. Azaiez *et al.*, Eur. Phys. J. A **15**, 93 (2002); A.N. Wilson, C.W. Beausang, N. Amzal, D.E. Appelbe, S. Asztalos, P.A. Butler, R.M. Clark, P. Fallon, A.O. Macchiavelli, Eur. Phys. J. A **9**, 183 (2000); R.V.F. Janssens *et al.*, Phys. Lett. B **546**, 55 (2002); J. Koenig *et al.*, Phys. Rev. C **24**, 2076 (1981).
22. G. Duchêne, F.A. Beck, P.J. Twin, G. de France, D. Curien, L. Han, C.W. Beausang, M.A. Bentley, P.J. Nolan, J. Simpson, Nucl. Instrum. Methods Phys. Res. A **432**, 90 (1999).
23. Ch. Droste, K. Starosta, A. Wierzchucka, T. Morek, S.G. Rohozinskii, J. Srebrny, M. Bergstrom, B. Herskind, E. Wesolowski, Nucl. Instrum. Methods Phys. Res. A **337**, 430 (1999).
24. K. Starosta *et al.*, Nucl. Instrum. Methods Phys. Res. A **423**, 16 (1999).
25. P. Datta *et al.*, Phys. Rev. C **69**, 044317 (2002).
26. W.S. Gray, T. Wei, J. Jänecke, R.M. Polichar, Phys. Lett. B **26**, 383 (1968).
27. N.G. Puttaswamy, J.L. Yntema, Phys. Rev. **177**, 1624 (1969).
28. W.S. Gray, P.J. Ellis, T. Wei, R.M. Polichar, J. Jänecke, Nucl. Phys. A **140**, 494 (1970).
29. J.W. Olness, W.R. Harris, A. Gallmann, F. Jundt, D.E. Alburger, D.H. Wilkinson, Phys. Rev. C **3**, 2323 (1971).
30. E.A. Samworth, J.W. Olness, Phys. Rev. C **5**, 1238 (1972).
31. A. Hogenbirk, H.P. Blok, M.G.E. Brand, A.G.M. Van Hees, J.F.A. Van Hienen, F.A. Jansen, Nucl. Phys. A **516**, 205 (1990).
32. B.A. Brown, A. Etchegoyen, W.D.M. Rae, N.S. Godwin, computer code OXBASH, 1984.
33. D.R. Goosman, C.N. Davids, D.E. Alburger, Phys. Rev. C **8**, 1324 (1973).
34. F. Ajzenberg-Selove, E.R. Flynn, S. Orbesen, J.W. Sunier, Phys. Rev. C **15**, 1 (1977).
35. A.M. Nathan, D.E. Alburger, Phys. Rev. C **15**, 1448 (1977).
36. F. Pellegrini, P. Guazzoni, D. Sinclair, E. Garman, Phys. Rev. C **16**, 1878 (1977).
37. B.V. Pritychenko, T. Glasmacher, B.A. Brown, P.D. Cottle, R.W. Ibbotson, K.W. Kemper, H. Scheit, Phys. Rev. C **62**, 051601(R) (2000).
38. J. Keinonen, R. Rascher, M. Uhrmacher, N. Wüst, K.P. Lieb, Phys. Rev. C **14**, 160 (1976).
39. Data extracted using the NNDC on-line Data Services from ENSDF, XUNDL and lifetime databases.
40. In another calculation for the negative-parity states, which allows $1\hbar\omega$ excitation to the pf shell, and without lowering the SPEs of the pf orbitals, the 3^- level comes just below the 4^- state. (B.A. Brown, private communication.)